Drug Design, Development and Therapy

Dovepress
open access to scientific and medical research

Open Access Full Text Article

ORIGINAL RESEARCH

Structural Insight into the Mechanism of 4-Aminoquinolines Selectivity for the alpha2A-Adrenoceptor

This article was published in the following Dove Press journal:
Drug Design, Development and Therapy

Zaibing Li,[1,2,*] Jingyu Li,[1,*] Liyan Liu,[1] Wenyi Deng,[3] Qingrong Liu,[4] Ruofan Liu,[4] Wen Zhang,[3] Zaiqing He,[5] Lei Fan,[6] Yingzhuo Yang,[7] Yun Duan,[7] Huifang Hou,[1] Xinyuan Wang,[1] Zhimei Yang,[1] Xiaoying Wang,[1] Shanze Chen,[1] Yi Wang,[1] Ning Huang,[1] Junli Chen[1]

[1]Department of Pathophysiology, West China School of Basic Medical Sciences & Forensic Medicine, Sichuan University, Chengdu 610041, People's Republic of China; [2]Department of Pathophysiology, School of Basic Medical Science, Southwest Medical University, Luzhou, Sichuan 646000, People's Republic of China; [3]West China Medical School, Sichuan University, Chengdu 610041, People's Republic of China; [4]West China School of Basic Medical Sciences & Forensic Medicine, Sichuan University, Chengdu 610041, People's Republic of China; [5]Department of Pathology, Nuclear of Industry 416 Hospital, Chengdu, Sichuan 610051, People's Republic of China; [6]Department of Occupational Medicine, Nuclear of Industry 416 Hospital, Chengdu, Sichuan 610051, People's Republic of China; [7]Department of Nuclear Medicine, Sichuan Cancer Hospital, Chengdu 610041, People's Republic of China

*These authors contributed equally to this work

Correspondence: Junli Chen; Ning Huang
Email chenjunlinsf@163.com; ninghuangcjl@163.com

Background: α_{2A}-adrenoceptor (AR) is a potential target for the treatment of degenerative diseases of the central nervous system, and α_{2A}-AR agonists are effective drugs for this condition. However, the lack of high selectivity for α_{2A}-AR subtype of traditional drugs greatly limits their clinic usage.

Methods: A series of homobivalent 4-aminoquinolines conjugated by two 4-aminoquinoline moieties via varying alkane linker length (C2-C12) were characterized for their affinities for each α_2-AR subtype. Subsequently, docking, molecular dynamics and mutagenesis were applied to uncover the molecular mechanism.

Results: Most 4-aminoquinolines (4-aminoquinoline monomer, C2-C6, C8-C10) were selective for α_{2A}-AR over α_{2B}- and α_{2C}-ARs. Besides, the affinities are of similar linker length-dependence for each α_2-AR subtype. Among all the compounds tested, C10 has the highest affinity for α_{2A}-AR (pKi=−7.45±0.62), which is 12-fold and 60-fold selective over α_{2B}-AR and α_{2C}-AR, respectively. Docking and molecular dynamics suggest that C10 simultaneously interacts with orthosteric and "allosteric" sites of the α_{2A}-AR. The mutation of F205 decreases the affinity by 2-fold. The potential allosteric residues include S90, N93, E94 and W99.

Conclusion: The specificity of C10 for the α_{2A}-AR and the potential orthosteric and allosteric binding sites proposed in this study provide valuable guidance for the development of novel α_{2A}-AR subtype selective compounds.

Keywords: alpha2-adrenoceptor, selectivity, linker length, allosteric modulation

Introduction

alpha2 adrenoceptors (α_2-ARs) belong to class A rhodopsin-like G-protein-coupled receptors, which are sub-classified to α_{2A}, α_{2B} and α_{2C}-ARs. α_2-ARs are mainly coupled to Gi protein and inhibit adenylyl cyclase activity, resulting in lower cAMP levels.[1]

α_2-ARs have been gradually recognized as promising antipsychotic therapeutic targets, especially for those associated with affective, psychotic, and cognitive symptoms.[2] α_{2A}-AR is widely distributed in the central nervous system (CNS), accounting for 90% of α_2-ARs, and is associated with regulation and strengthen of memory, analgesia, sedation, and has an anti-epileptic effect.[3] Thus, the activation of the α_{2A}-AR can improve the clinic symptoms of CNS degenerative diseases. However, increasingly more studies have shown that α_{2A}-AR and α_{2C}-AR have different or even opposing roles in the CNS.[4] For instance, the activation of the α_{2A}-AR ameliorates spatial working memory ability of mice, while the activation of the α_{2C}-AR destroys

submit your manuscript | www.dovepress.com
DovePress
http://doi.org/10.2147/DDDT.S214157

this ability.[4] These studies indicate that the selective α_{2A}-AR agonists might be one of the most ideal treatments for CNS degenerative diseases. However, the lack of highly selective α_{2A}-AR compounds limits the development of α_{2A}-AR selective drugs and their clinical use.

In previous studies, homobivalent 4-aminoquinoline compounds (Figure 1A) were shown to have nanomolar affinity for the α_2-AR when the three subtypes of the α_2-AR had not been discovered, and the affinities had tissue-specific differences.[5,6] In addition, the affinities were of linker-length dependence, suggesting there might be a second pocket that is different from the orthosteric pocket (endogenous agonist binding site). Any site on a receptor that is distinct from the orthosteric site is called allosteric site.[7] The development of allosteric modulators has drawn increasingly more attention due to their several potential advantages over traditional (orthosteric) drugs, including having higher subtype selectivity and maintaining spatiotemporal patterns of physiological signaling, etc.[7] It has been confirmed that α_2-ARs have three subtypes and have different tissue distributions.[1] The above results suggest that homobivalent 4-aminoquinoline compounds with certain linker lengths might have higher affinity for a certain subtype of α_2-ARs, which might partly be resulted from the allosteric interaction.

In the current study, a series of homobivalent 4-aminoquinoline compounds with different linker length (2–12) were synthesized and their affinities for each α_2-AR subtype were measured via radioligand binding assays as previously described.[8] Molecular docking, molecular dynamics and site-directed mutagenesis studies were then carried out to investigate the interacting sites of 4-aminoquinolines with α_{2A}-AR.

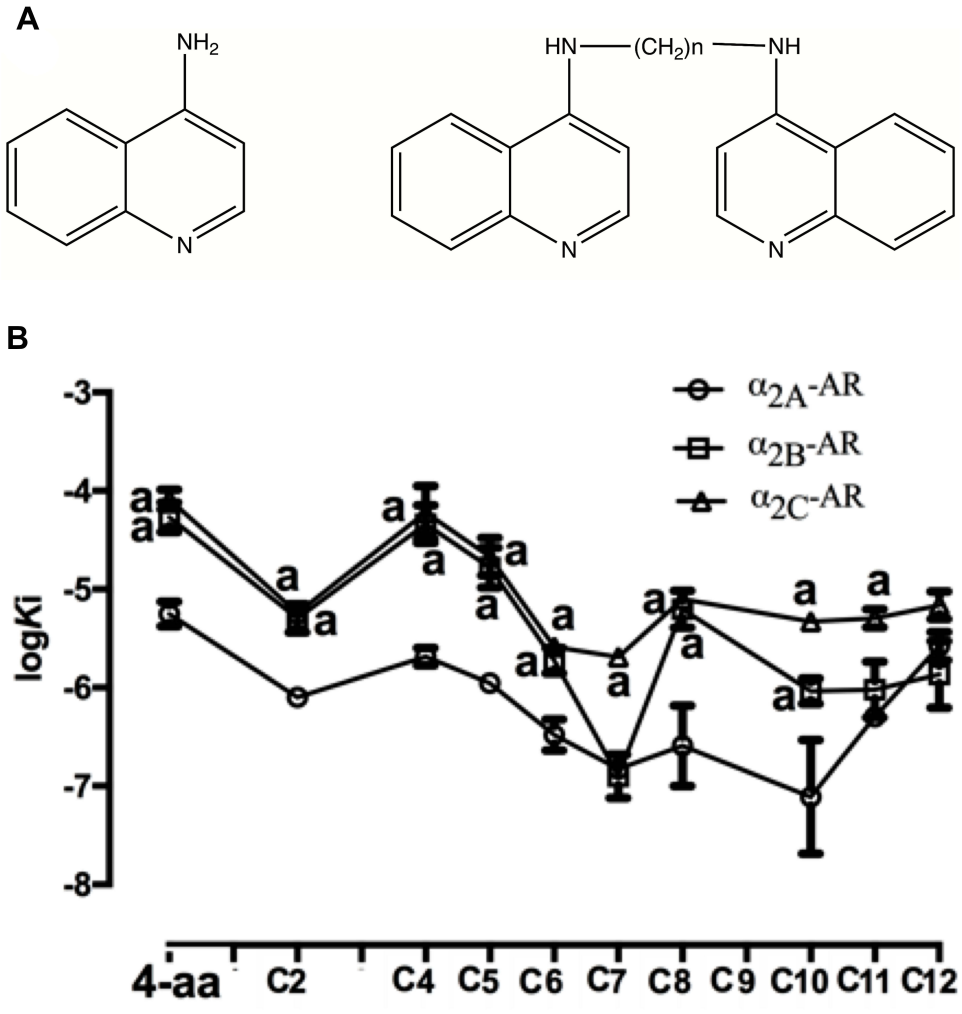

Figure 1 Structures (**A**) and subtype selective binding (**B**) of 4-aminoquinoline compounds. (**A**) n represents the number of methylene groups in the linking chain. (**B**) Competition binding assay was performed on membranes prepared from α_{2A}, α_{2B} or α_{2C}-ARs transiently transfected COS-7 cells. All binding curves were fit by a one-site binding model. Affinities were compared using one-way ANOVA and student-Newman-Keuls multiple comparison tests. a: $p<0.05$ compared to 4-aminoquinoline, b: $p<0.05$ compared to α_{2A}-AR.

Materials and Methods

Materials

COS-7 cells were purchased from ATCC (Manassas, VA, USA). DEAE-Dextran kit was bought from Beyotime Biotechnology (Shanghai, China). [^{125}I]-paraiodoclonidine (PIC) was from PerkinElmer (Waltham, MA, USA). MEM media, Lipofectamine 2000 were from Invitrogen (Carlsbad, CA, USA). IBMX, forskolin, phentolamine, norepinephrine, 1,4-butanediamine, 1,5-diamino-pentane, 1,6-hexanediamine, 1,7-diaminoheptane, 1,8-O[1]ktandiamin, 1,10-Diaminodecane, 1,11-Diaminoundecane, and 1,12-Diaminododecane were from Sigma-Aldrich (St. Louis, MO, USA). Plasmid mini Kit I, Endo-Free Plasmid Maxi Kit were from Omega (Norcross, GA, USA). DMT Enzyme, cAMP-GlO^{TM} Assay kit were from Promega (USA). Human α_{2A}-AR, α_{2B}-AR and α_{2C}-AR in pcDNA3.1^{+} were from Missouri S&T cDNA Resource Center (www.cdna.org).

Synthesis

A series of homobivalent 4-aminoquinoline compounds connected by alkane linkers of varying lengths were synthesized as previously described.[9] All 4-aminoquinolines were dissolved in dimethyl sulphoxide (DMSO). These stock solutions were stored at −80°C.

Cell Culture, Transient Transfection and Membrane Preparations

COS-7 cells were cultured in DMEM supplemented with 10% fetal bovine serum and 1% penicillin/streptomycin. Transient transfection of human α_{2A}-, α_{2B}-, and α_{2C}-ARs in pcDNA3.1^{+} vectors was performed using the method described previously.[10] Briefly, 1x10^{7} COS-7 cells were seeded per 150 mm plate and transfected 24 hrs later using 14 μg plasmid DNA per plate. 48–72 hrs later, cells were scraped into cold PBS, and centrifuged at 500g for 4 mins at 4°C. The pellet was resuspended in 20 mL of cold solution (20 mM HEPES, 10mM EDTA, pH 7.4). They were disrupted by homogenization for 10 seconds using an ultra-turrax homogenizer at 24,000 rpm, with an interval of 30 seconds between each homogenization. The homogenate was centrifuged at 1300g for 10 mins at 4°C and the supernatant was centrifuged at 40,000g for 1 hr at 4°C. The membrane pellet was resuspended in 0.6-1mL buffer (50 mM Tris-HCl, 120 mM sucrose, pH 7.4, and 10% glycerol (v/v)). The membrane suspension was homogenized on ice using an insulin syringe, aliquoted and stored at −80°C. The protein concentration was determined using Bradford reagent.

Site-Directed Mutagenesis

Site-directed mutagenesis was carried out through PCR reaction to mutate the potential orthosteric and allosteric sites of the α_{2A}-AR to alanine (A). Primers were shown in supplementary information Table S1. PCR reaction was performed using the gold mix kit, and samples were subjected to 30 cycles of 10 seconds of denaturation at 98°C, 10 seconds of annealing at 55°C, and 7 mins of elongation at 72°C. A DMT restriction enzyme was used to digest the parental plasmid. The constructed mutant plasmids were transformed into DH5α competent cells. The positive colony with the mutant plasmids was identified by sequencing.

Radioligand Binding Assays

All ligands and membranes were suspended in buffer containing 50 mM Tris-HCl and 120 mM sucrose. Receptor expression assay was performed to determine the appropriate protein concentration used for future binding assays. Increasing concentrations of membranes containing each α_2-AR subtype were incubated with 400 pM of [^{125}I]-PIC in a total volume of 200 μL. Non-specific binding was defined as binding in the presence of 100 μM phentolamine. A concentration of membrane was chosen when it provided an adequate total binding compared to non-specific binding and the bound was less than 10% of the total radioligand added. For saturation binding assay, membranes containing each α_2-AR subtype were incubated with various concentrations of ^{12I}-PIC (0.1–10 nM) in a total volume of 200 μL. For competition binding assay, 4–15 μg of each α_2-AR subtype membranes were incubated with 400 pM of [^{125}I]-PIC and increasing concentrations of test compounds in a total volume of 200 μL. Non-specific binding was defined as binding in the presence of 100 μM phentolamine. All the reaction mixtures for all binding experiments were incubated at room temperature for 1 hr, and the reaction was terminated by PBS and vacuum filtration through GF/B filters. Radioactivity was measured by a [^{125}I] beta counter.

cAMP Assay

The production of intracellular cAMP was determined using cAMP-GlO^{TM} Assay kit. Briefly,1x10^{5} cells mL^{-1} of transiently transfected COS-7 cells were seeded into 96 well plates and cultured for 48 hrs. Cells were then washed with DMEM and were treated for 30 mins with 20 μL DMEM containing 1 mM IBMX, 30 μM forskolin and different concentrations (10^{-10}-10^{-3} M) of test compounds. Cells

were lysed for 30 mins at room temperature in cAMP-Glo lysis buffer (20 μL per well). 40 μL/well detection solution (containing PKA substrate and PKA holoenzyme) was added and cultured at room temperature for 20 min. 80 μL/well of Kinase-Glo™ Regent was added, which were cultured for 10 mins at room temperature. Luminescence was measured with luminometers.

Homology Modeling

The human α_{2A}-AR sequence obtained from the uniport database was used to screen the experimentally modeled protein structure and the human β1-AR (PDB ID: 2YCY) crystal structure was selected as the template. The homology model of the α_{2A}-AR was built using the sequence alignment of α_{2A}-AR and β1-AR via SWISS-MODEL server. The predicted 3D structure of the α_{2A}-AR was further optimized by MODELLER (v9.16), which was then evaluated using ERRAT plot and Ramachandran plot.

Molecular Docking

Molecular docking was performed using Autodock vina to investigate the binding mode between 4-aminoquinolines and the α_{2A}-AR. The search grid of the α_{2A}-AR was identified as center_x: 18.16, center_y: 20.7, center_z: −6.67 with dimensions size_x: 100, size_y: 100, and size_z: 100. All other parameters were set as "default". The best-scoring pose as judged by the Vina docking score was chosen and visually analyzed using Accelrys Discovery Studio Client version 3.1 (Accelrys Software Inc. USA).

Molecular Dynamics (MD) Simulations

The MD simulations were performed in a hydrated dipalmitoyl phosphatidylcholine (DPPC) bilayer using the GROMACS (version 2016) software package.[11] CHARMM36 force field[12] was used for protein and lipid, and CGenFF force field[13] was used for small molecules. The system was heated to 300k for 5 ns in NVT ensemble. Subsequently, the equilibration simulation ran for 10 ns in NPT ensemble (Pressure=1atm and temperature=300k). Finally, the production simulation was conducted for 50 ns. RMSD and C-αRMSF analyses were performed to monitor the stability of the system, and the binding-free energy was calculated via MM/PBSA software.

Data Analysis

Nonlinear regression analysis of saturation, competition binding, and inositol phosphate accumulation assay data was performed using GraphPad Prism 6.0 (San Diego, CA, USA). Statistically significant differences ($p<0.05$) between the affinities of all compounds were compared using one-way ANOVA and student-Newman-Keuls multiple comparison tests.

Results and Discussion

The Affinity of 4-Aminoquinolines at α_2-ARs

Synthesis of 4-Aminoquinolines

A series of 4-aminoquinolines with different linker lengths (2–12) shown in Figure 1A were synthesized as described previously.[9] All synthesized compounds were identified by proton nuclear magnetic resonance and mass spectrometry (Supplementary materials, Figure S1&S2).

Determination of the Affinity of 4-Aminoquinolines at α_2-ARs

To address subtype selectivity of 4-aminoquinolines, their apparent affinities were evaluated on membrane-expressed human α_2-ARs via competition radioligand binding assays using [^{125}I]-PIC (α_{2A}-AR K_D= 0.2090±0.06 nM, α_{2B}-AR K_D= 0.6020±0.081 nM, α_{2C}-AR K_D= 0.8023±0.053 nM).

In general, 4-aminoquinoline compounds showed nano- to sub-micromolar affinities for the three α_2-AR subtypes (Figure 1B, Table 1). Most 4-aminoquinoline compounds had greater affinity than the 4-aminoquinoline monomer for each α_2-AR subtype (Figure 1B, Table 1), suggesting that conjugation of two 4-aminoquinoline pharmacophores can increase the affinity for the α_2-ARs. This is consistent with previous studies.[14] The 4-aminoquinoline and homobivalent 4-aminoquinolines with linker lengths between 2–6, and 8–10 carbons showed a 6–24 fold selectivity for α_{2A}-AR over α_{2B}-AR ($p<0.05$); and all the 4-aminoquinoline compounds, were of 2.6–60 fold selectivity for α_{2A}-AR over α_{2C}-AR ($p<0.05$), suggesting that the molecular size of these 4-aminoquinoline compounds can fit better for the ligand-binding site of the α_{2A}-AR.

There is a similar linker length–affinity relationship for each α_2-AR subtype. At the α_{2A}-AR, there are two domains of high affinity for 4-aminoquinolines, that is when the linkage comprises 2 and 10 methylene groups (Figure 1B, Table 1). Specifically, C2 had an affinity of 797 nM, which decreased when the linker length was increased to 4 or 5 (Figure 1B, Table 1). We speculated that C2 has the most suitable size to fit the binding pocket of the α_{2A}-AR, and therefore forms more interactions with the receptor. In contrast, the size of 4-aminoquinolie is too small, while that of C4 and C5 is too big which might lead to steric clashes,

Table 1 Binding Affinities of Homobivalent 4-Aminoquinolines for α_2-ARs

Compound	α_{2A}-AR			α_{2B}-AR			α_{2C}-AR		
	p*Ki*	*Ki*(nM)	n	p*Ki*	*Ki*(nM)	n	p*Ki*	*Ki*(nM)	n
4-aminoquinoline	−5.25±0.12	5596	3	−4.27±0.15[b]	53,790	3	4.09±0.10[b]	81,470	3
C2	6.10±0.07	797	3	−5.30±0.14[b]	5075	3	−5.24±0.06[b]	5750	3
C4	−5.69±0.09	2062	3	−4.34±0.19[b]	45,870	3	−4.22±0.27[b]	60,440	3
C5	−5.96±0.06	1109	3	−4.78±0.20[b]	16,560	3	−4.67±0.19[b]	21,320	3
C6	−6.52±0.18	329.4	3	−5.73±0.13[b]	1883	3	−5.59±0.04[b]	2585	3
C7	−6.83±0.03	149	3	−6.90±0.22	126	3	−6.69±0.04[b]	2042	3
C8	−6.78±0.44	259	3	−5.20±0.19[b]	6266	3	−5.10±0.08[b]	7898	3
C10	−7.45±0.62	78	3	−6.04±0.13[b]	923	3	−5.33±0.01[b]	4697	3
C11	−6.30±0.01	506	3	−6.02±0.28	951	3	−5.29±0.09[b]	5080	3
C12	−5.58±0.15	2640	3	−5.87±0.34	1354	3	−5.16±0.14	6857	3

Notes: All data presented are the mean±SE of separate assays, performed in duplicate.*Ki* refers to the concentration of ligand required to occupy 50% of unoccupied receptors, calculated according to the Cheng-Prusoff equation: $Ki=IC_{50}/1+([L]/K_D)$ where [L] is the radioligand concentration and K_D is the dissociation constant.p*Ki* is the negative log of the *Ki* value.[a]$p<0.05$ compared to 4-aminoquinoline. [b]$p<0.05$ compared to α_{2A}-AR.

resulting in decreased affinity. Interestingly, the affinity increased afterwards when the linker of homobivalent 4-aminoquinoline compounds was further lengthened, reaching at the peak at 10 (78 nM) carbon atoms, which decreased thereafter when the linker was further lengthened to 11 and 12 (Figure 1B, Table 1). We hypothesized that the linker length of 6–10 is of appropriate length for the compounds to interact with the residues that are located at the extracellular surface of the receptor. The homobivalent 4-aminoquinoline compounds had a similar trend of linker length–affinity relationship for α_{2B}-AR and α_{2C}-AR, but the peak was located at C2 (α_{2B}-AR, 5075; α_{2C}-AR 5750 nM) and C7 (α_{2B}-AR, 125 nM; α_{2C}-AR, 2042 nM) (Figure 1B, Table 1).

The Effect of C10 on the Production of cAMP

α_2-ARs are mainly coupled to Gαi protein and inhibit adenylyl cyclase to produce cAMP. However, α_2-ARs could also increase cAMP accumulation by either activating adenylyl cyclase II or under lower agonist concentrations.[15,16]

To define the effect of C10 on cAMP production in COS-7 cells, cAMP accumulation assay was carried out by testing the effect of C10 on forskolin induced activation of α_{2A}-AR. C10 showed a biphasic effect on cAMP production in COS-7 cells expressing the α_{2A}-AR. At lower concentrations (10^{-10}-10^{-7} M), C10 increased cAMP production, whereas at higher concentrations (10^{-6}-10^{-4} M) inhibited cAMP accumulation (Figure 2A). This biphasic effect is similar to previously reported results with epinephrine in CHO cells, which showed an inhibition effect from 10^{-9} to 10^{-8} M, and an increase from 10^{-7} to 10^{-6} M.[16] In COS-7 cells, we have also shown that norepinephrine inhibited the production of cAMP at lower concentrations (10^{-10}-10^{-8}M), while stimulated the expression of cAMP at higher concentrations (10^{-3}-10^{-7}M) (Figure 2B). As reported previously,[16] phentolamine, a known antagonist of the α_{2A}-AR, did not have any effect on the production of cAMP (Figure 2C), but suppressed NA to produce cAMP, with an IC50 value of 97.05±0.086 nM (Figure 2D).

The Interactions Predicted by Molecular Docking

Construction and Optimization of α_{2A}-AR Homology Model

Given that 4-aminoquinoline monomer and C10 showed specificity for α_{2A}-AR, and C10 had the highest affinity for the α_{2A}-AR among all 4-aminoquinolines, their possible interacting sites were predicted via molecular docking. The α_{2A}-AR homology model was firstly constructed based on the β1-AR (PDB ID: 2YCY) template via swiss-model. The predicted 3D structure was further optimized by MODELLER (v9.16), which was then evaluated using ERRAT plot and Ramachandran plot. The ERRAT program gave a score of 90.862, and the results of the Ramachandran plot showed that 97% of residues were in the most favored and allowed regions, indicating a good quality model.

Molecular Docking

Molecular docking results showed that 4-aminoquinoline monomer formed a hydrogen bond with D113 (TMIII) (Figure 3A), which has been shown to be a conserved

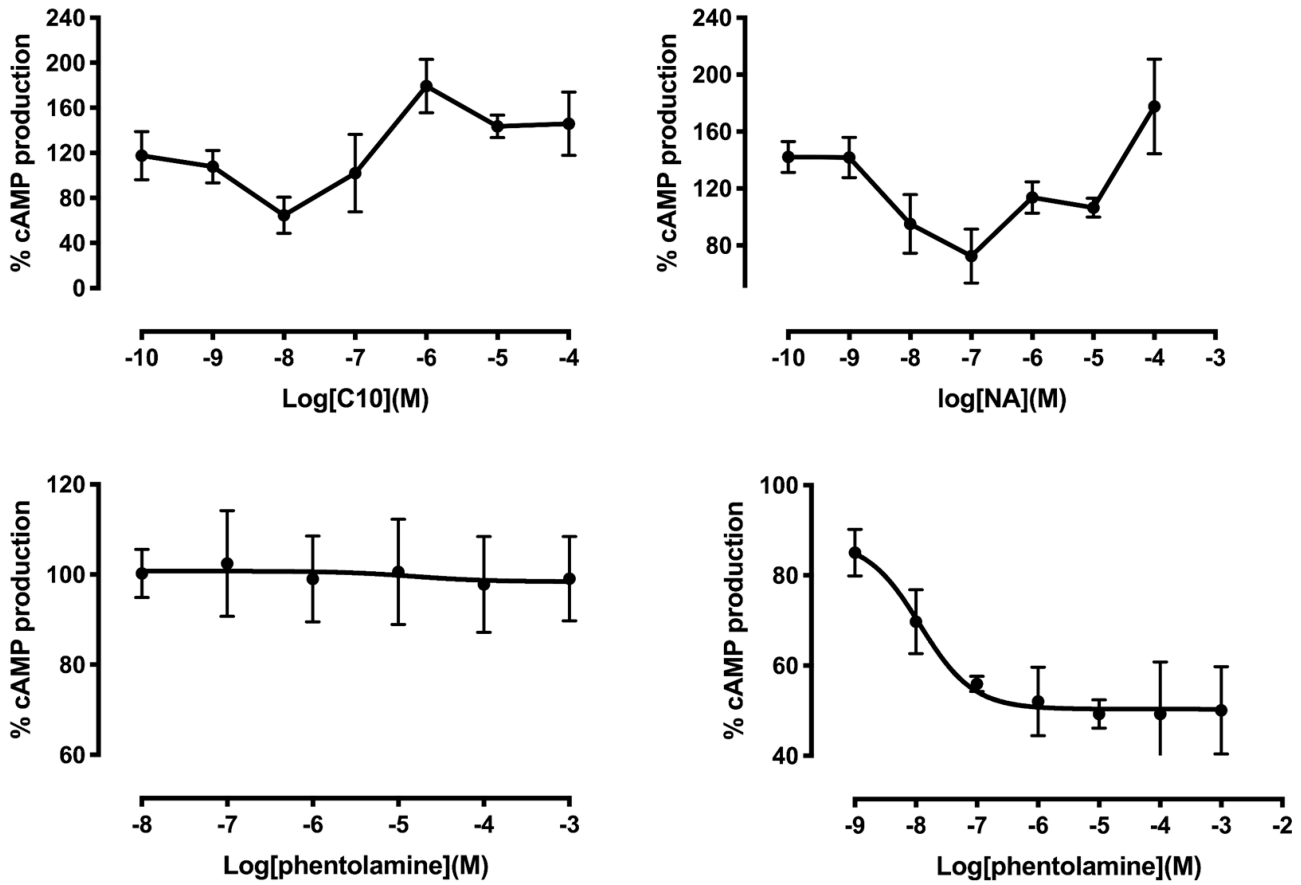

Figure 2 The effect of C10 on forskolin induced cAMP accumulation. COS-7 cells transiently transfected with α_{2A}-AR were treated for 30 mins at 37°C with 20 μL DMEM containing 1 mM IBMX, 30 μM forskolin and increasing concentrations of C10 (**A**), norepinephrine (**B**), phentolamine (**C**), phentolamine and 10^{-4} M norepinephrine (**D**). cAMP concentration was monitored with luminometers. Points represent the mean percentage of forskolin response.

orthosteric residue (endogenous agonist binding site) among aminergic GPCRs.[17] The results suggest that 4-aminoquinoline monomer is situated at the orthosteric binding pocket of the α_{2A}-AR. Interestingly, one quinoline moiety of C10 is within the orthosteric binding pocket, forming a π-π interaction with W387, while the other quinoline ring is located at the extracellular surface of the receptor, forming a π-π interaction with W99 (ECL1) and a hydrogen bond with C106 (TMIII) (Figure 3B, Figure S3, Figure S4).

The Interactions Predicted by Molecular Dynamics Simulations

Molecular Dynamics Simulations

A 50 ns molecular dynamics simulation was carried out to further validate the reliability of the docking results between 4-aminoquinolines and the α_{2A}-AR. The root-mean-square deviation (RMSD) of each system showed that the α_{2A}-AR docked with either 4-aminoquinoline monomer or C10 achieved equilibrium at around 20 ns with RMSD average value of approximately 0.8 nm and 1 nm, respectively (Figure 3C). The root-mean-square fluctuation (RMSF) profiles were then analyzed to investigate the fluctuations of residues with the conformational transition. We found that the 4-aminoquinoline monomer-α_{2A} and C10-α_{2A} complexes had very similar RMSF profiles. The RMSF was around 1.1 nm at the extracellular and intracellular loops, and was less than 0.5 nm for other residues, suggesting the loops are relatively more fluctuant than the alpha helices and beta sheets (Figure 3D).

Calculation of Binding-Free Energy

The binding-free energy of the protein-compound complexes was calculated using MM/PBSA method. 4-aminoquinoline monomer demonstrated negative binding-free energy value of −111.69 KJ/mol, while C10 possessed value of −289.70 KJ/mol, indicating C10 has higher affinity for the α_{2A}-AR than the 4-aminoquinoline monomer. This is in a good agreement with the *K*i values of our competitive binding assays, which supports the reliability of our force field parameters and MD simulations.

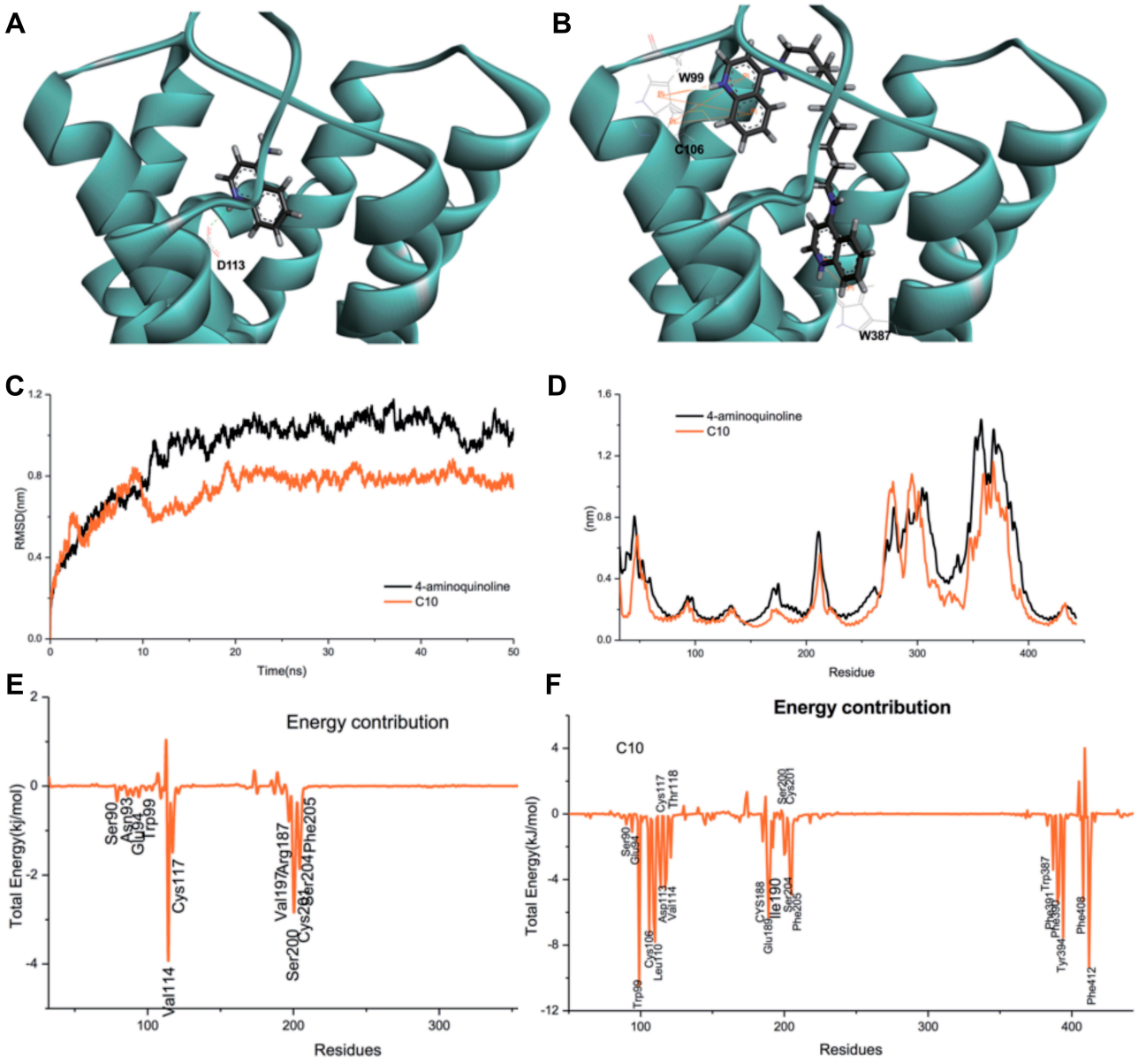

Figure 3 The interactions between 4-aminoquinoles and the α_{2A}–AR. 4-aminoquinoline monomer (**A**) or C10 (**B**) were docked into the α_{2A} -AR homology based on a human β1-AR crystal structure (2YCY). Molecular dynamics was subsequently performed. The root-mean-square deviation (RMSD) was shown in (**C**), and the root-mean-square fluctuation (RMSF) profiles were in (**D**). And each residue energy contribution to the binding-free energy of the system was in (**E**) (4-aminoquinoline- α_{2A} -AR) and (**F**) (C10-α_{2A} -AR).

Estimation of the Contribution of Key Residues to the Binding-Free Energy

g_mmpbsa was applied to determine each residue contribution to the binding-free energy to determine the key residues interacting with the 4-aminoquinolines. Figure 3E and Table S2 demonstrated that the key residues of the 4-aminoquinoline-α_{2A} complex that contributed to the total free energies were located at TMIII (V114, C117), TMV (V197, S200, C201, S204, F205), TMVI (W387, F390, F391, Y394), TMVII (F412), ECL2 (R187). Interestingly, some residues which are located at the extracellular part of TMⅡ or ECL1, also contributed to the binding-free energy but with lower energies, including S90 (TMⅡ,-0.27 KJ/mol), N93 (TMⅡ,-0.06 KJ/mol), E94 (TMⅡ,-0.35 KJ/mol), and W99 (ECL1, −0.13 KJ/mol) (Figure 3E, Table S2).

C10-α_{2A} complex had very similar features to 4-aminoquinoline-α_{2A} complex but with higher energy contributions of each residue. The key residues of the C10-α_{2A} complex that contributed more than 2 KJ/mol were located at TMIII (C106, Y109, L110, D113, V114, C117, T118), TMⅤ (S200, C201, S204, F205), TMⅥ (W387, F390, F391, Y394), TMⅦ (F408, F412, F413), ECL2 (C188, E189, I190)

(Figure 3F, Table S2). Similar to 4-aminoquinoline-α_{2A} complex, some residues in the C10-α_{2A} complex at the extracellular part of TMⅡ or ECL1 also contributed to the binding-free energy with lower energies, including E94 (TMⅡ, −1.10 KJ/mol), S90 (TMⅡ, −0.64 KJ/mol), N93 (TMⅡ, −0.53 KJ/mol) and W99 (ECL1, −10.48 KJ/mol) (Figure 3F, Table S2).

The endogenous agonist binding pocket of aminergic GPCRs is called the orthosteric site. It has been shown previously that Ser200, Cys201, Ser204 of the α_{2A}-AR interact with catecholamines, and are involved in the activation of the receptor,[18] suggesting S200, C201 and S204 are located at the orthosteric binding site of the α_{2A}-AR. The interaction of 4-aminoquinoline and C10 with these three resides indicate that 4-aminoquinoline and C10 are within the orthosteric binding pocket of the α_{2A}-AR. Besides, our results show that the key residues that contribute to the total free energies are located at the transmembrane regions of helixes III, Ⅴ, Ⅵ, Ⅶ, and ECL2, which are consistent with the reported orthosteric binding pocket of aminergic GPCRs.[19,20]

The development of allosteric modulators has been shown to be an effective way to obtain subtype selective ligands.[7] Previous studies have suggested that there is a "common" allosteric site among different aminergic GPCRs, which comprises the residues from ECL2 and the extracellular part of TMII and TMVII.[21,22] In the present study, molecular dynamics simulations of both 4-aminoquinoline-α_{2A} and C10-α_{2A} complexes demonstrate that some residues which are located at ECLI or the extracellular part of TMII also contributed to the total free energies, including W99 (ECLI), S90, N93 and E94 (TMII). These results suggest that W99, S90, N93 and E94 might be allosteric sites of the α_{2A}-AR. The lower energies contributed by the potential allosteric sites compared to the orthosteric residues could be due to the fact that allosteric modulators normally have lower affinities than the orthosteric ligands.[22] The interaction of one 4-aminoquinoline moiety with the allosteric site might cause the structural changes of the α_{2A}-AR, thus leading to the higher affinity and selectivity of C10 for the α_{2A}-AR.

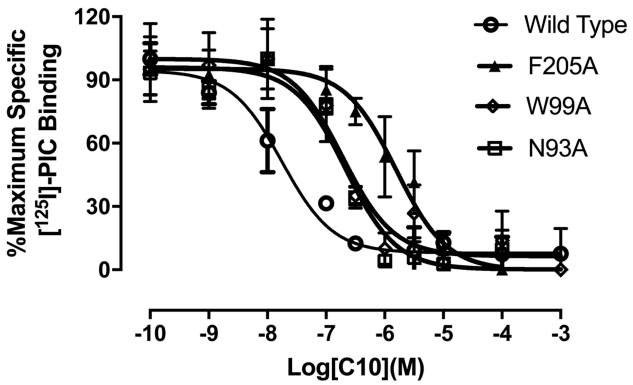

Figure 4 Competitive binding affinity of C10 for α_{2A} -AR mutants. Competition by C10 for specific binding of 400pM [^{125}I]-PIC to membranes prepared from wild type α_{2A}-AR (○), or α_{2A}-AR mutants, F205A (▲), W99A (◊), or N93A (□) transfected COS-7 cells. Points are mean percentage of maximum specific binding and vertical bars represent standard error. Curves were best fit to a single-site model. Affinities were compared using one-way ANOVA and student-Newman-Keuls multiple comparison tests.

F205A Decreased the Affinity of C10 for the α_{2A}-AR

In order to investigate the molecular mechanism of the specificity of C10 for the α_{2A}-AR, two potential orthosteric residues (E189, F205) and allosteric sites (N93, W99) predicted by molecular dynamics simulations, were selected and mutated to alanine. Subsequently, competition binding assay was performed to investigate the effect of the mutants on the affinity of C10 for the α_{2A}-AR. We found that F205A reduced the affinity by 2-fold (Figure 4, Table 2), indicating F205 plays an important role during the interaction of C10 and the α_{2A}-AR.

N93 and W99 are potential allosteric sites of the α_{2A}-AR predicted by our docking and dynamics studies. However, both N93A and W99A increased the affinity by 1.5-, 1.7-fold, respectively, instead of decreasing the affinity for C10 (Figure 4, Table 2). This could be because that both N93 and W99 are not truly the binding site of C10. However, the mutation of these two residues to a relatively smaller, and unchanged residue (A), may cause the conformational changes

Table 2 Binding Affinities of C10 for α_{2A}-AR Mutants

Compound	α2A–AR			E189A			F205A			N93A			W99A		
	*p*Ki	*Ki*(nM)	n	*p*Ki	*Ki*(nM)	n	*p*Ki	*Ki*(nM)	n	*p*Ki	*Ki*(nM)	n	*p*Ki	*Ki*(nM)	n
C10	−6.69 ±0.55	202	3	−6.57 ±0.08	280	3	−6.40 ±0.45	394	3	−6.88 ±0.05	134	3	−6.94 ±0.20	116	3

Notes: All data presented are the mean±SE of separate assays, performed in duplicate. *Ki* refers to the concentration of ligand required to occupy 50% of unoccupied receptors, calculated according to the Cheng-Prusoff equation: $Ki=IC_{50}/1+([L]/K_D)$ where [L] is the radioligand concentration and K_D is the dissociation constant. *p*Ki is the negative log of the *Ki* value.

of the receptor, therefore, leading to an increased affinity of C10 as discussed in previous studies.[23] Mutation of other residues suggested by docking and molecular dynamics simulation studies should be performed in the near future.

Conclusion

In this study, we demonstrated that homobivalent 4-aminoquinolines have a higher affinity for the α_{2A}-AR over α_{2B}-, α_{2C}-ARs. Specifically, C10 has the highest affinity for the α_{2A}-AR among all the 4-aminoquinolines and F205 has been confirmed to be one of the interacting sites. Most importantly, we have for the first time proposed the potential allosteric site of the α_{2A}-AR. This study will provide valuable structural information for the development of novel α_{2A}-AR subtype selective compounds.

Abbreviations

AR, Adrenoceptor; CNS, Central nervous system; [^{125}I]-PIC, [^{125}I]-paraiodoclonidine.

Acknowledgments

This work was supported by National Science Foundation of China Grant (81803648, 81470931, 31401188, 31701098, 81803183), Sichuan University Grant (2018SCUH0039, 2016SCU11021, 2016SCU04A08) and Applied Basic Research Program of Sichuan Province Grant (2016JY0027).

Disclosure

The authors declare no conflicts of interest in this work.

References

1. Fallarero A, Pohjanoksa K, Wissel G, et al. High-throughput screening with a miniaturized radioligand competition assay identifies new modulators of human alpha2-adrenoceptors. *Eur J Pharm Sci*. 2012;47(5):941–951. doi:10.1016/j.ejps.2012.08.021
2. Brosda J, Jantschak F, Pertz HH. alpha2-adrenoceptors are targets for antipsychotic drugs. *Psychopharmacology (Berl)*. 2014;231(5):801–812. doi:10.1007/s00213-014-3459-8
3. Uys MM, Shahid M, Harvey BH. Therapeutic potential of selectively targeting the alpha2C-adrenoceptor in cognition, depression, and schizophrenia-new developments and future perspective. *Front Psychiatry*. 2017;8:144. doi:10.3389/fpsyt.2017.00144
4. Scheinin M, Sallinen J, Haapalinna A. Evaluation of the alpha2C-adrenoceptor as a neuropsychiatric drug target studies in transgenic mouse models. *Life Sci*. 2001;68(19–20):2277–2285. doi:10.1016/S0024-3205(01)01016-5
5. Adams A, Jarrott B, Elmes BC, Denny WA, Wakelin LP. Interaction of DNA-intercalating antitumor agents with adrenoceptors. *Mol Pharmacol*. 1985;27(4):480–491.
6. Adams A, Jarrott B, Denny WA, Wakelin LP. Differences between central and peripheral rat alpha-adrenoceptors revealed using binuclear ligands. *Eur J Pharmacol*. 1986;127(1–2):27–35. doi:10.1016/0014-2999(86)90202-5
7. Conn PJ, Lindsley CW, Meiler J, Niswender CM. Opportunities and challenges in the discovery of allosteric modulators of GPCRs for treating CNS disorders. *Nat Rev Drug Discov*. 2014;13(9):692–708. doi:10.1038/nrd4308
8. Höcker J, Weber B, Tonner PH, et al. Meperidine, remifentanil and tramadol but not sufentanil interact with α2-adrenoceptors in α2A-, α2B- and α2C-adrenoceptor knock out mice brain. *Eur J Pharmacol*. 2008;582(1–3):70–77. doi:10.1016/j.ejphar.2007.12.022
9. Deshpande SM, Singh AK. Synthesis of some N,N'-bis-(9-acridino)-, -diaminoalkanes dihydrochloride as potential antibacterial, antitubercular and antileprotics. *Chem Pharm Bull (Tokyo)*. 1972;20(1):206–208. doi:10.1248/cpb.20.206
10. Lopata MA, Cleveland DW, Sollner-Webb B. High level transient expression of a chloramphenicol acetyl transferase gene by DEAE-dextran mediated DNA transfection coupled with a dimethyl sulfoxide or glycerol shock treatment. *Nucleic Acids Res*. 1984;12(14):5707–5717. doi:10.1093/nar/12.14.5707
11. Abraham MJ, Murtola T, Schulz R, et al. GROMACS: high performance molecular simulations through multi-level parallelism from laptops to supercomputers. *SoftwareX*. 2015;1–2:19–25. doi:10.1016/j.softx.2015.06.001
12. Lee J, Cheng X, Swails JM, et al. CHARMM-GUI input generator for NAMD, GROMACS, AMBER, OpenMM, and CHARMM/OpenMM simulations using the CHARMM36 additive force field. *J Chem Theory Comput*. 2016;12(1):405–413. doi:10.1021/acs.jctc.5b00935
13. Kim S, Lee J, Jo S, Brooks CL 3rd, Lee HS, Im W. CHARMM-GUI ligand reader and modeler for CHARMM force field generation of small molecules. *J Comput Chem*. 2017;38(21):1879–1886. doi:10.1002/jcc.v38.21
14. Lensing CJ, Freeman KT, Schnell SM, Adank DN, Speth RC, Haskell-Luevano C. An in vitro and in vivo investigation of bivalent ligands that display preferential binding and functional activity for different melanocortin receptor homodimers. *J Med Chem*. 2016;59(7):3112–3128. doi:10.1021/acs.jmedchem.5b01894
15. Federman AD, Conklin BR, Schrader KA, Reed RR, Bourne HR. Hormonal stimulation of adenylyl cyclase through Gi-protein beta gamma subunits. *Nature*. 1992;356(6365):159–161. doi:10.1038/356159a0
16. Wade SM, Lan K, Moore DJ, Neubig RR. Inverse agonist activity at the alpha(2A)-adrenergic receptor. *Mol Pharmacol*. 2001;59(3):532–542. doi:10.1124/mol.59.3.532
17. Nyronen T, Pihlavisto M, Peltonen JM, et al. Molecular mechanism for agonist-promoted alpha(2A)-adrenoceptor activation by norepinephrine and epinephrine. *Mol Pharmacol*. 2001;59(5):1343–1354. doi:10.1124/mol.59.5.1343
18. Peltonen JM, Nyronen T, Wurster S, et al. Molecular mechanisms of ligand-receptor interactions in transmembrane domain V of the alpha2A-adrenoceptor. *Br J Pharmacol*. 2003;140(2):347–358. doi:10.1038/sj.bjp.0705439
19. Surgand JS, Rodrigo J, Kellenberger E, Rognan D. A chemogenomic analysis of the transmembrane binding cavity of human G-protein-coupled receptors. *Proteins*. 2006;62(2):509–538. doi:10.1002/prot.20768
20. Kooistra AJ, Kuhne S, De Esch IJ, Leurs R, De Graaf C. A structural chemogenomics analysis of aminergic GPCRs: lessons for histamine receptor ligand design. *Br J Pharmacol*. 2013;170(1):101–126. doi:10.1111/bph.12248
21. Dror RO, Pan AC, Arlow DH, et al. Pathway and mechanism of drug binding to G-protein-coupled receptors. *Proc Natl Acad Sci U S A*. 108(32):13118–13123. doi:10.1073/pnas.1104614108
22. Haga K, Kruse AC, Asada H, et al. Structure of the human M2 muscarinic acetylcholine receptor bound to an antagonist. *Nature*. 2012;482(7386):547–551. doi:10.1038/nature10753
23. Zhang L, Anderson RJL, Ahmed I, et al. Manipulating cofactor binding thermodynamics in an. artificial oxygen transport protein. *Biochemistry*. 2011;50(47):10254–10261. doi:10.1021/bi201242a